Semisegmented Amphiphilic Polymer Conetworks: Synthesis and Characterization

Demetris Kafouris,[†] Michael Gradzielski,[‡] and Costas S. Patrickios*[,†]

Department of Chemistry, University of Cyprus, P.O. Box 20537, 1678 Nicosia, Cyprus, and Stranski-Laboratorium für Physikalische and Theoretische Chemie, Institut für Chemie, Strasse des 17. Juni 124, Sekr. TC7, Technische Universität Berlin, D-10623 Berlin, Germany

Received December 25, 2008; Revised Manuscript Received February 18, 2009

ABSTRACT: Semisegmented amphiphilic polymer conetworks (APCNs) based on the hydrophilic monomer 2-(dimethylamino)ethyl methacrylate (DMAEMA), the hydrophobic monomer methyl methacrylate (MMA), and the hydrophobic cross-linker ethylene glycol dimethacrylate (EGDMA) were prepared using group transfer polymerization in a two-step procedure that involved the synthesis of linear polyDMAEMA or polyMMA arms, followed by their cross-linking using a mixture of EGDMA with either MMA or DMAEMA, respectively. Four semisegmented APCNs with polyMMA arms with degrees of polymerization (DPs) of 10, 20, 30, and 40 and three with polyDMAEMA arms with DPs of 10, 20, and 30 were prepared. The sol fraction extracted from the APCNs, the percentage of linear polymer in the sol fraction, and the molecular weights of the branched fraction of the extractables increased as the DP of the arms increased. The degrees of swelling (DSs) in water of all semisegmented APCNs increased with decreasing pH and increasing percentage of DMAEMA hydrophilic units. Despite the rather imperfect, semisegmented placement of the dissimilar units, extensive small-angle neutron scattering (SANS) experiments in D_2O indicated that nanophase organization did take place within these APCNs and persisted, in many cases, even at full ionization of the hydrophilic monomer repeating units. The SANS profiles were also used to calculate the spacings between the scattering centers, which were found to increase with the content in the DMAEMA units and their degree of ionization.

Introduction

Chemical (covalent) amphiphilic polymer conetworks (APCNs)[1] represent an emerging class of novel materials, whose synthesis, characterization, and evaluation for applications constitute the research focus of several polymer teams around the world.[2] APCNs are composed of hydrophilic and hydrophobic units, covalently interlinked into a 3D structure. When each type of units is present in sufficiently long sequences, APCNs are internally organized into two nanophases, one hydrophilic and one hydrophobic.[3] In this case, each nanophase can function independently by favorably interacting with molecules of like polarity. This leads to swelling in nanophase-compatible solvents and adsorption of like solutes. The rich functional behavior of APCNs renders them appropriate materials for a range of applications, including drug release,[4] tissue engineering,[5] enzyme immobilization,[6] synthesis of mesoporous silica,[7] growth of semiconducting nanocrystals,[8] soft contact lenses,[9] pervaporation membranes,[10] extractants of organic solvents from water,[11] temperature-activated actuators,[11] biochemical sensors,[12] and phase transfer catalysts.[13]

Although these applications do not require conetwork structural perfection, the preparation of model[14] APCNs represents an important synthetic target that is necessary for the derivation of accurate structure−property relationships. For the past nine years, our research team has been working on the development of synthetic strategies for the preparation of quasi-model APCNs characterized by high degrees of homogeneity in chain length and composition and a distribution in the number of arms at the cross-linking nodes.[15] In particular, we have been using two controlled polymerization methods, group transfer polymerization (GTP)[16] and reversible addition−fragmentation chain transfer (RAFT) polymerization[17] for the development of quasi-model APCNs of two different topologies: regular APCNs in which all chains are, in principle, end-linked,[18] and cross-linked star APCNs bearing an equal number of end-linked and singly attached (i.e., dangling) chains.[19] The structures with these two topologies are illustrated schematically in Figure 1a,b.

In an effort to investigate the effect of the degree of structural perfection of APCNs on their self-assembly, in this study we prepared and characterized semisegmented APCNs. These materials had a structural perfection intermediate between that of our quasi-model APCNs and that of conventional, randomly cross-linked APCNs. In particular, the present semisegmented APCNs had one well-defined linear segment, either the hydrophilic or the hydrophobic, which was prepared first. The second comonomer (the hydrophobic or the hydrophilic, respectively) was not introduced as a well-defined linear segment, but, instead, it formed the main body of the conetwork with the cross-linker with which it was simultaneously copolymerized in the second and final synthetic step. This approach represents a simplification of our previously developed methodologies for the preparation of end-linked APCNs and cross-linked star APCNs by the merging of synthetic steps and their reduction from 3 and 4, respectively, down to 2, as illustrated in Figure 1.

The semisegmented APCNs were prepared by GTP to secure rapid and quantitative polymerizations and to control the molecular weight of the segments. The resulting APCNs were characterized in terms of their degrees of swelling (DSs) in water as a function of the degree of ionization of the weakly basic hydrophilic units and in tetrahydrofuran (THF). Furthermore, the extent of nanophase separation was explored using small-angle neutron scattering (SANS) experiments on APCNs swollen in deuterium oxide containing various amounts of deuterium chloride effecting different degrees of ionization of the hydrophilic units.

Experimental Section

Materials. 2-(Dimethylamino)ethyl methacrylate (DMAEMA, 98%), methyl methacrylate (MMA, 99%), ethylene glycol dimethacry-

* To whom correspondence should be addressed. E-mail: costasp@ucy.ac.cy.
[†] University of Cyprus.
[‡] Technische Universität Berlin.

10.1021/ma802859d CCC: $40.75
Published on Web 04/01/2009

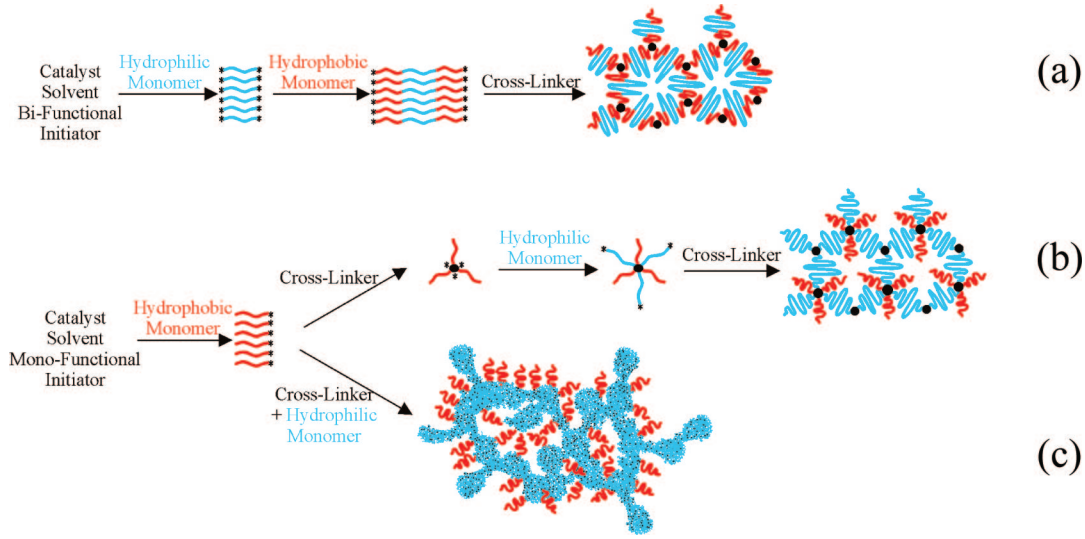

Figure 1. Schematic representation of the synthesis of the three different types of quasi-model conetworks prepared: (a) regular, (b) cross-linked star, and (c) semisegmented.

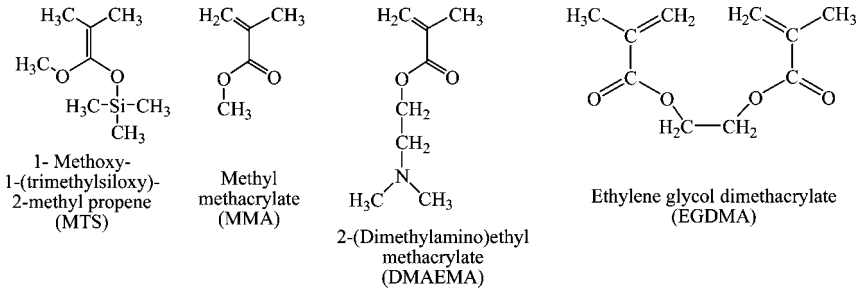

Figure 2. Chemical structures and names of the main reagents used for the polymer conetwork synthesis: the monofunctional initiator MTS, the monomers MMA and DMAEMA, and the cross-linker EGDMA.

late (EGDMA, 98%), 1-methoxy-1-trimethylsiloxy-2-methyl propene (MTS, 95%), tetrabutylammonium hydroxide (40% w/w in water), benzoic acid (99.5%), and 2,2-diphenyl-1-picrylhydrazyl hydrate (DPPH, 95%) were all purchased from Aldrich, Germany. THF was purchased from Labscan, Ireland, and was used as the mobile phase in chromatography (HPLC grade) and as a solvent (reagent grade) for the polymerizations. The chemical structures and names of the main reagents used for the conetwork synthesis are shown in Figure 2.

Methods. The polymerization solvent, THF, was dried by refluxing over a potassium−sodium amalgam for 3 days and was freshly distilled prior to use. The polymerization catalyst, tetrabutylammonium bibenzoate (TBABB), was synthesized by the reaction of tetrabutylammonium hydroxide and benzoic acid in water, following the procedure of Dicker et al.,[16c] and was kept under vacuum until use. DMAEMA, MMA, and EGDMA were passed through basic alumina columns to remove protic impurities and polymerization inhibitors. They were subsequently stirred over calcium hydride (to remove the last traces of moisture and protic impurities) in the presence of added DPPH free-radical inhibitor and stored in the refrigerator at about 5 °C. Finally, they were freshly distilled under vacuum just before their use and kept under a dry nitrogen atmosphere. The initiator was distilled once prior to the polymerization, but it was neither contacted with calcium hydride nor passed through basic alumina columns because of the risk of hydrolysis. All glassware was dried overnight at 120 °C and assembled hot under dynamic vacuum prior to use.

Polymer Synthesis. Polymer synthesis was performed using GTP,[16] a "living" polymerization method, which secured well-defined polymer structures in a rapid and quantitative polymerization. The synthesis consisted of two sequential polymerization steps. In the first step, one of the two monomers was polymerized, yielding the conetwork arms. In the second step, a mixture of the cross-linker with the second monomer was simultaneously copolymerized, resulting in the formation of the main body of the conetwork. Therefore, two different types of semisegmented APCNs were prepared in this study. One with polyMMA arms and a poly(DMAEMA-*co*-EGDMA) body and one with polyDMAEMA arms and a poly(MMA-*co*-EGDMA) body. In each type, the arm length was systematically varied at a constant volume and composition of the cross-linking mixture. PolyMMA arms covering the range of degrees of polymerization (DPs) from 10 to 40 and polyDMAEMA arms of DPs of 10, 20, and 30 were prepared. It is noteworthy that an attempted APCN with a polyDMAEMA arm of DP 40 would not form a conetwork, but it instead provided a star copolymer. Figure 3 summarizes the synthetic sequences employed.

The polymerization procedure for the synthesis of one of the APCNs is detailed below. To a 100 mL round-bottomed flask containing a small amount (∼10 mg) of TBABB were syringed 44 mL of freshly distilled THF and 0.3 mL MTS initiator (0.26 g, 1.47 mmol), in this order, followed by the slow addition of 1.6 mL of MMA (1.49 g, 14.7 mmol) under stirring. The polymerization exotherm (24.4−32.9 °C) abated within 5 min, and a sample was extracted. In the second stage, 9.2 mL of the cross-linking mixture (7.5 mL of DMAEMA (6.99 g, 44.3 mmol) and 1.7 mL of EGDMA (1.78 g, 8.85 mmol)) was added, which promoted gelation within 2 min.

Characterization of the Polymer Solutions. *Gel Permeation Chromatography.* The molecular weights (MWs) and the molecular weight distributions (MWDs) of the star copolymer, the linear precursors to the conetworks and to the star copolymer, and the extractables from the conetworks were determined by gel permeation chromatography (GPC) using a single Polymer Laboratories PL-mixed "D" column. The mobile phase was THF (flow rate 1 mL min^{-1}), delivered using a Waters 515 HPLC pump. The refractive index (RI) signal was measured using an ERC-7515A RI detector supplied by Polymer Laboratories. (This chromatography system is to be called

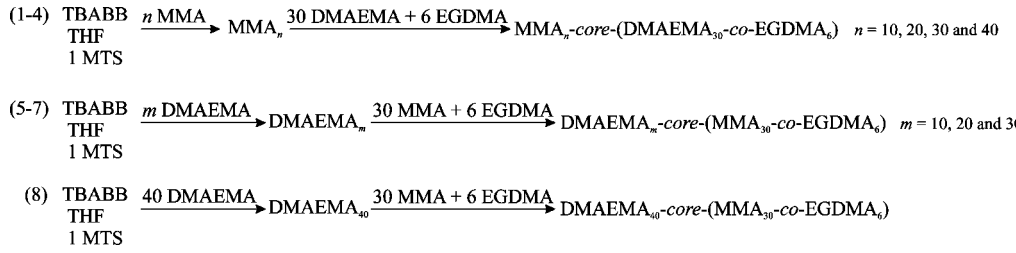

Figure 3. Synthetic sequences employed for the preparation of the copolymers of this study.

GPC-RI.) The calibration curve was based on eight narrow MW (630, 2680, 4250, 13 000, 28 900, 50 000, 128 000 and 260 000 g mol^{-1}) linear polyMMA standards supplied by Polymer Laboratories, which provided accurate MW calculations for the linear precursors but only a qualitative estimate for the MW of the star copolymer. In particular, the following quantities were calculated: the number-average MWs, M_n, the polydispersity indices (PDI, M_w/M_n, where M_w is the weight-average MW), and the peak MWs, M_p, which are the MWs at the peak maximum.

Static Light Scattering. The absolute M_w values of the star copolymer and the extractables from the conetworks were measured by static light scattering (SLS) in a flow system configuration (GPC-SLS) using a BI-MwA Brookhaven spectrophotometer equipped with a 30 mW red diode laser emitting at 673 nm and a multiangle detector determining the intensity of scattered light at seven different angles: 35, 50, 75, 90, 105, 130, and 145°. The mobile phase was THF (flow rate 1 mL min^{-1}), delivered using a Polymer Laboratories PL-LC1120 isocratic pump. Between the pump and the BI-MwA SLS detector, a single Polymer Laboratories PL-mixed "D" column was connected. The RI signal was measured using a Polymer Laboratories PL-RI 800 RI detector, connected after the SLS detector. The PSS-WinGPC 7 software was used for the MW calculations. The polymer samples were dissolved in HPLC-grade THF and were filtered through 0.45 μm pore size syringe filters. The RI increments (dn/dc) of the polymer solutions in THF were determined using an ABBE refractometer.

^{1}H NMR Spectroscopy. The star copolymer and the extractables from the conetworks were characterized using proton nuclear magnetic resonance (^{1}H NMR) spectroscopy in deuterated chloroform ($CDCl_3$). The spectra were recorded using a 300 MHz Avance Bruker spectrometer equipped with an ultrashield magnet.

Dynamic Light Scattering. The hydrodynamic size of the star copolymer in a 1% w/w solution in THF was measured by dynamic light scattering (DLS) using a 90Plus Brookhaven spectrophotometer with Particle Sizing software version 2.31, equipped with a 30 mW red diode laser operating at 673 nm. The measurement was performed at an angle of 90° and at room temperature. The measurement lasted 1 h. The data were processed using a multimodal size distribution analysis based on non-negatively constrained least-squares (NNCLS). Prior to the light scattering measurement, the polymer solution was filtered through a 0.45 μm PTFE syringe filter three times to remove any existing dust particles.

Small-Angle Neutron Scattering. The radius of gyration of the star copolymer in 1% w/w solution in d_6-DMSO was measured using SANS. The SANS measurements were performed using the spectrometer PAXE at the Laboratoire Léon Brillouin (LLB, CEA-CNRS, Saclay, France) with a neutron wavelength of 6 Å and sample-to-detector distances of 1.055 and 4.055 m, thereby covering a range of magnitude of the scattering vector, q, of 0.009 to 0.33 Å^{-1}. The solution of the star copolymer was contained in a 2 mm Hellma quartz cuvette. The sensitivity of the individual detector elements was accounted for by comparing it with the scattering of a water (H_2O) sample in a 1 mm thick quartz cuvette. The data were recorded on a 64 × 64 2D detector and afterward were radially averaged, corrected for the transmission values, and converted into absolute scattering intensities by comparison with the intensity of the incident beam via a standard procedure.[20] The background scattering of the empty cell and the electronic background were subtracted during this correction procedure; that is, the obtained data contained only the coherent and incoherent scattering of the sample. We performed the analysis of the SANS data of the star copolymer by fitting the model of Gaussian starlike polymers[21] to the whole scattering curve $I(q)$. For this model, the scattering intensity is given by eq 1

$$I(q) = c_g \frac{MW}{N_A rho^2}(\rho_p - \rho_s)^2 \frac{2}{fx^2}\left[x - (1 - e^{-x}) + \frac{f-1}{2}(1 - e^{-x})^2\right] \quad \text{with} \quad x = \frac{f}{3(f-2)}q^2R_g^2 \quad (1)$$

Here c_g is the mass concentration of the star copolymer, f is its number of arms, N_A is the Avogadro's number, *rho* is the density of the copolymer, and ρ_p and ρ_s are the scattering length densities of the copolymer and the solvent, respectively. For ρ_p and ρ_s, we employed values of 9.4 × 10^9 and 52.8 × 10^9 cm^{-2}, respectively, which resulted from the identical densities of the copolymer and of d_6-DMSO of 1.19 g mL^{-1}.

Atomic Force Microscopy. A dilute sample solution of the star copolymer (0.1 mg mL^{-1} in chloroform) was spin-coated on a graphite surface and was subsequently visualized by atomic force microscopy (AFM). AFM imaging was performed on a PicoPlus scanning probe microscope from Molecular Imaging (Agilent) using a cantilever (Applied Nanostructures; length: 125 μm; width: 45 μm; resonant frequency: 200−400 kHz; force constant: 25−75 N m^{-1}; tip radius <10 nm, height: 12−16 μm). The measurement was carried out with tapping mode at room temperature in the air.

Network Characterization. *Determination of the Sol Fraction (Extractables) of the APCNs.* We took the conetworks out of the polymerization flasks by breaking the flasks. Subsequently, they were transferred to glass bottles, where they were washed in 200 mL of THF for 1 week to remove the sol fraction. The THF solution was then recovered by filtration, and the solvent was removed using a rotary evaporator. The sol fraction was calculated as the ratio of the mass of the dried extracted polymer to the theoretical dry mass of the conetwork, estimated as the sum of the masses of the monomer, the cross-linker, plus the initiator used for the conetwork synthesis. The extractables were characterized in terms of their MW and composition using GPC-RI, GPC-SLS, and ^{1}H NMR, as previously described.

Characterization of the Degree of Swelling of the APCNs. The DSs of the conetworks were measured in THF, pure water, and aqueous solutions of various pHs covering the range between 2 and 11. The DSs were calculated as the ratio of the swollen divided by the dry conetwork mass. All masses were determined gravimetrically. First, the swollen masses of fifteen cubic samples (edge size 5−10 mm; each sample was in a separate glass vial) from each conetwork were measured after equilibration for 2 weeks in THF. Next, we determined the dry mass of each sample after removing the THF by placing all samples in a vacuum oven at room temperature for 8 days. Then, 5 mL of milli-Q (deionized) water was added to each vial. For each conetwork, nine of its samples were acidified by the addition of a calculated volume of a 0.5 M HCl standard solution such that degrees of ionization between 11 and 99% were achieved. The calculation was based on the measured dry mass of each sample (from which the number of equivalents of the DMAEMA units was estimated) and the assumption that all DMAEMA units were not ionized before the addition of HCl. The pHs of these nine samples covered the range of 4−7. Three more samples from each conetwork were further acidified to cover the pH range of 2 to 3.5, two samples became

Table 1. Molecular Weight Characteristics of the Linear Precursors to the APCNs as Measured Using GPC-RI

network chemical formula[a]	theoretical MW	GPC-RI on linear precursors		
		M_p (g mol^{-1})	M_n (g mol^{-1})	M_w/M_n
$DMAEMA_{10}$-*core*-(MMA_{30}-*co*-$EGDMA_6$)	1672	2310	1690	1.27
$DMAEMA_{20}$-*core*-(MMA_{30}-*co*-$EGDMA_6$)	3244	4020	3260	1.15
$DMAEMA_{30}$-*core*-(MMA_{30}-*co*-$EGDMA_6$)	4816	7010	5830	1.13
MMA_{10}-*core*-($DMAEMA_{30}$-*co*-$EGDMA_6$)	1100	2830	1940	1.30
MMA_{20}-*core*-($DMAEMA_{30}$-*co*-$EGDMA_6$)	2100	4940	4250	1.14
MMA_{30}-*core*-($DMAEMA_{30}$-*co*-$EGDMA_6$)	3100	7010	5770	1.13
MMA_{40}-*core*-($DMAEMA_{30}$-*co*-$EGDMA_6$)	4100	10600	9050	1.12

[a] *core*: precedes the contents of the core of the APCNs.

Table 2. Size Characteristics of the Star Copolymer as Determined Using a Variety of Techniques

polymer chemical formula[a]	theoretical MW	GPC-RI results			GPC-SLS results		SANS	DLS	AFM
		M_p (g mol^{-1})	M_n (g mol^{-1})	M_w/M_n	M_w (g mol^{-1})	no. arms	R_g (nm)	R_h (nm)	R (nm)
$DMAEMA_{40}$	6380	8610	7060	1.20	–	–	–	–	–
$DMAEMA_{40}$-*core*-(MMA_{30}-*co*-$EGDMA_6$)	–	43 000	34 000	1.20	158 000	12	20.7	22.1	26.0

[a] *core*: precedes the contents of the core of the star copolymer.

alkaline (pH 9−11) by the addition of small volumes of a 0.5 M NaOH standard solution, and the last sample remained neutral (no acid or base was added to it, just the 5 mL of deionized water) and had a pH of 7 to 8. The samples were allowed to equilibrate for 2 weeks, and the solution pH and swollen conetwork mass were measured. All aqueous DSs were determined in triplicate, and the averages of the measurements are presented along with the 95% confidence intervals. The DSs in THF and in the aqueous environment were calculated as the ratio of the swollen conetwork mass in THF or water, respectively, divided by the dry conetwork mass.

Calculation of the Degree of Ionization and the pK. The degree of ionization of each sample was calculated as the number of added HCl equivalents divided by the number of DMAEMA unit equivalents (calculated from the conetwork dry mass and conetwork composition) present in the sample. We obtained the hydrogen ion titration curves by plotting the calculated degrees of ionization against the measured solution pH. The effective pK of the DMAEMA units of each conetwork was estimated from the hydrogen ion titration as the solution pH at 50% ionization.

Small-Angle Neutron Scattering. The structure of all APCNs swollen in D_2O at different degrees of ionization of the DMAEMA monomer repeating units, 0, 50, and 100%, effected by the addition of the appropriate volume of a DCl solution in D_2O, was probed by SANS using the same spectrometer and instrument configuration as those used for the characterization of the R_g of the star copolymer described in a previous paragraph. The APCN samples were contained in Hellma quartz cuvettes of 1 mm thickness. The rather irregular shapes of the conetwork pieces did not allow the homogeneous filling of the cuvettes. This, in turn, implied that the obtained scattered intensities would depend on the percentage of material in the beam, which was not exactly the same for all samples.

Results and Discussion

Polymer Synthesis. The synthesis of the semisegmented APCNs comprised successful, two-step, sequential additions in a one-pot preparation (summarized in Figure 1c) and was based on the ability of GTP to produce well-defined linear polymers upon the addition of a methacrylate monomer to a THF solution of monofunctional initiator and catalyst and the interconnection of these linear polymers upon the addition of a cross-linking mixture of EGDMA and monomer. If the polymer chain produced in the first step is sufficiently short, then interconnection in step two leads to network formation. In the opposite case, star polymers are obtained. That is why the preparation with the longest polyDMAEMA arms consistently yielded star copolymers. Figure 1c shows that the well-defined linear homopolymer chains formed in the first synthetic step would constitute the dangling chains of the final semisegmented APCN product. The main continuous body of the APCN is the product of the random copolymerization of the cross-linker and the second comonomer, taking place in the second and final synthetic step.

Characterization of the Polymer Solutions. *Molecular Weights.* Table 1 lists the chemical formulas of all of the APCNs prepared in this study and the MW characteristics of their linear arm precursors, as determined by GPC-RI. The M_n values of the linear polymers were higher than the theoretical values because of partial initiator deactivation. Their MWDs were unimodal and relatively narrow. Whereas the PDIs of the linear arms with DPs of 10 were reasonably low (∼1.3), those with higher DPs were lower than 1.15, in qualitative agreement with the predictions of Poisson distribution, applicable to "living" polymers, and dictating a better size homogeneity for larger polymers.[22] The PDIs of the present linear polymers that were higher than what Poisson distribution would dictate are due to the limitations of GTP arising from its quasi-livingness.

Figure 4 shows the GPC-RI signal for the star copolymer $DMAEMA_{40}$-*core*-(MMA_{30}-*co*-$EGDMA_6$) and its linear precursor. Whereas the MWD of the linear DMAEMA homopolymer precursor was narrow and unimodal, as expected, that of the star copolymer was bimodal and also contained an amount of unattached linear chains in addition to the star. Table 2 shows the data from the GPC-RI and GPC-SLS MW characterization of the star copolymer. The apparent GPC-RI M_n of the star copolymer was 34 000 g mol^{-1} and was much lower than the absolute one because of the compact nature of the star structure compared with the linear polyMMA MW calibration standards. The absolute M_w of the star copolymer as determined by GPC-SLS, also shown in Table 2, was 158 000 g mol^{-1}, which is almost 5 times higher than the GPC-RI M_n. We calculated the absolute number of arms of the star copolymer by dividing the

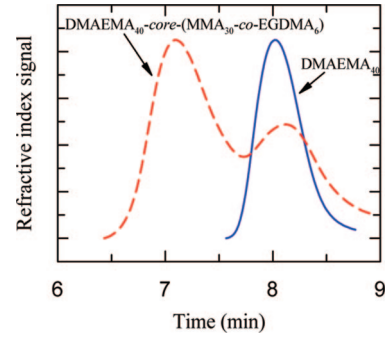

Figure 4. GPC traces of the star copolymer $DMAEMA_{40}$-*core*-(MMA_{30}-*co*-$EGDMA_6$) and its linear precursor $DMAEMA_{40}$.

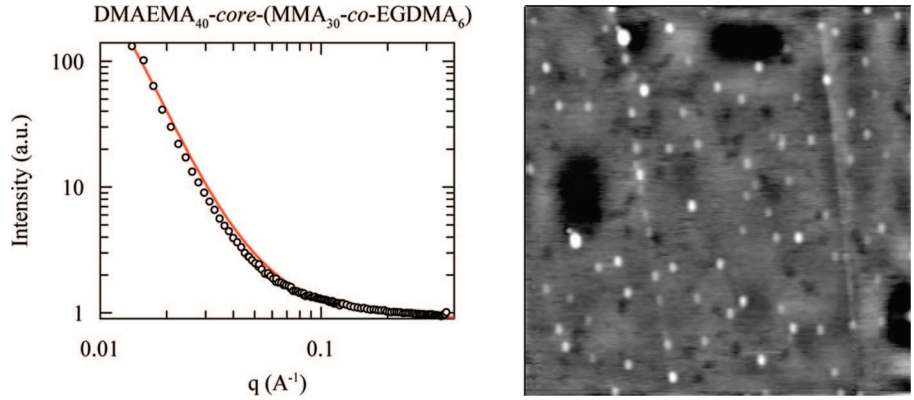

Figure 5. Left: Small-angle neutron scattering (SANS) profile for the star copolymer at 1% w/w concentration in d_6-DMSO. The solid line is the fit according to eq 1. Right: AFM topography image of the star copolymer. Image size: 3 × 3 μm^2.

Table 3. Molecular Weight and Composition Characteristics of the Sol Fraction of the APCNs

			GPC results			SLS results[b]	% mol DMAEMA		
polymer chemical formula	w/w % extractables	% linear polymer	M_p (g mol^{-1})	M_n (g mol^{-1})	M_w/M_n	M_w (g mol^{-1})	experimental by ^{1}H NMR	theoretical of APCNs	corrected theoretical
DMAEMA$_{10}$-*core*-(MMA$_{30}$-*co*-EGDMA$_6$)	11.1	41.7	15 700	28 500	1.44	73 800	54.5	25	56.3
			1520	1130	1.27				
DMAEMA$_{20}$-*core*-(MMA$_{30}$-*co*-EGDMA$_6$)	12.8	63.7	70 200	64 100	1.28	180 300	75.7	40	78.2
			4210	3550	1.14				
DMAEMA$_{30}$-*core*-(MMA$_{30}$-*co*-EGDMA$_6$)	28.9	82.4	68 200	78 600	1.07	137 800	81.3	50	91.2
			7220	5760	1.18				
MMA$_{10}$-*core*-(DMAEMA$_{30}$-*co*-EGDMA$_6$)	6.5	52.1	9180	10 500	1.43	23 600	31.0	75	36.0
			1570	1020	1.33				
MMA$_{20}$-*core*-(DMAEMA$_{30}$-*co*-EGDMA$_6$)	6.6	84.0	14 800	16 800	1.34	26 500	5.7	60	9.6
			2860	2410	1.16				
MMA$_{30}$-*core*-(DMAEMA$_{30}$-*co*-EGDMA$_6$)	8.0	86.6	15 700	18 200	1.20	41 000	5.6	50	6.7
			3850	3170	1.17				
MMA$_{40}$-*core*-(DMAEMA$_{30}$-*co*-EGDMA$_6$)	11.0	100	6220	4960	1.18		0.0	43	0.0

[a] *core*: precedes the contents of the core of the APCNs. [b] Only the higher MW peak clearly visible in the GPC-SLS signal.

absolute M_w measured from GPC-SLS by the effective M_w of the arm (M_w of the linear precursor from GPC-RI plus the MW corresponding to the MMA and the EGDMA in the core), and it was found to be 12.

Radius of Gyration, Hydrodynamic Radius, and Adsorption Radius on Graphite Substrate. The size of the star copolymer in solution and upon adsorption on a surface was also investigated. Table 2 also summarizes the values of the radius of gyration (R_g), the hydrodynamic radius (R_h), and the adsorption radius (R) on graphite of the star copolymer, as determined by SANS, DLS, and AFM, respectively. Figure 5 presents the SANS data and the AFM image of the star copolymer.

The value of R_g calculated on the basis of the star model was found to be 20.7 nm, which is in good agreement with the value of R_h, 22.1 nm. The R value, 26 nm, was slightly higher than the values of R_h and R_g because of the flattening of the particles upon adsorption and because of the finite AFM tip size.

Network Characterization. *Sol Fraction.* Table 3 shows the sol fraction extracted from each conetwork. In most cases, the sol fraction was relatively low, below 13% w/w, with its value increasing with the DP of the arms, in agreement with previous studies[18e,f,h,i] and consistent with the fact that GTP is less "living" at higher MWs. The extractables were characterized by GPC-RI and GPC-SLS, and the results are also shown in Table 3. In all cases, the MW of the lower MW fraction of the extractables was close to the MW of the linear arm, suggesting that the former originated from unattached arms. With the exception of MMA$_{40}$-*core*-(DMAEMA$_{30}$-*co*-EGDMA$_6$), the sol fraction from the rest of the conetworks consisted of both star and linear polymers. The percentage of linear polymer in the sol fraction increased with the arm DP, with the lowest amount being as low as 40% and the highest amount being 100%. The MW of the high MW peak in the extractables, representing star polymers, also increased with the arm DP. Therefore, as the DP of the arms increased, both the sol fraction and the percentage of linear polymer within the sol fraction increased.

Table 4. Degrees of Swelling of the APCNs in THF and in Aqueous Solutions of Acidic and Basic pH

		degree of swelling		
polymer chemical formula[a]	% mol DMAEMA	THF	low pH	high pH
DMAEMA$_{10}$-*core*-(MMA$_{30}$-*co*-EGDMA$_6$)	25	8.2	4.4	2.5
DMAEMA$_{20}$-*core*-(MMA$_{30}$-*co*-EGDMA$_6$)	40	13.2	8.7	2.5
DMAEMA$_{30}$-*core*-(MMA$_{30}$-*co*-EGDMA$_6$)	50	20.7	19.4	3.4
MMA$_{10}$-*core*-(DMAEMA$_{30}$-*co*-EGDMA$_6$)	75	6.7	24.7	3.2
MMA$_{20}$-*core*-(DMAEMA$_{30}$-*co*-EGDMA$_6$)	60	6.9	22.6	3.1
MMA$_{30}$-*core*-(DMAEMA$_{30}$-*co*-EGDMA$_6$)	50	7.7	14.7	2.9
MMA$_{40}$-*core*-(DMAEMA$_{30}$-*co*-EGDMA$_6$)	43	7.9	7.1	2.3

[a] *core*: precedes the contents of the core of the APCNs.

The composition of the polymers in the sol fraction was determined using ^{1}H NMR. Table 3 shows the theoretical (corresponding to the theoretical conetwork composition based on the comonomer feed ratio), the "corrected theoretical", and the experimental DMAEMA compositions of the extractables. The "corrected theoretical" DMAEMA composition was calculated by using the percentages of linear and star fractions in the extractables (determined from the relative peak areas in the GPC-RI traces) and by assuming that the linear fraction consisted of pure homopolymer, whereas the star fraction had the theoretical composition of the conetwork. The experimental DMAEMA composition was calculated by the ratio of the characteristic peak of the DMAEMA units at 4.1 ppm (two protons) and the characteristic peak of the MMA

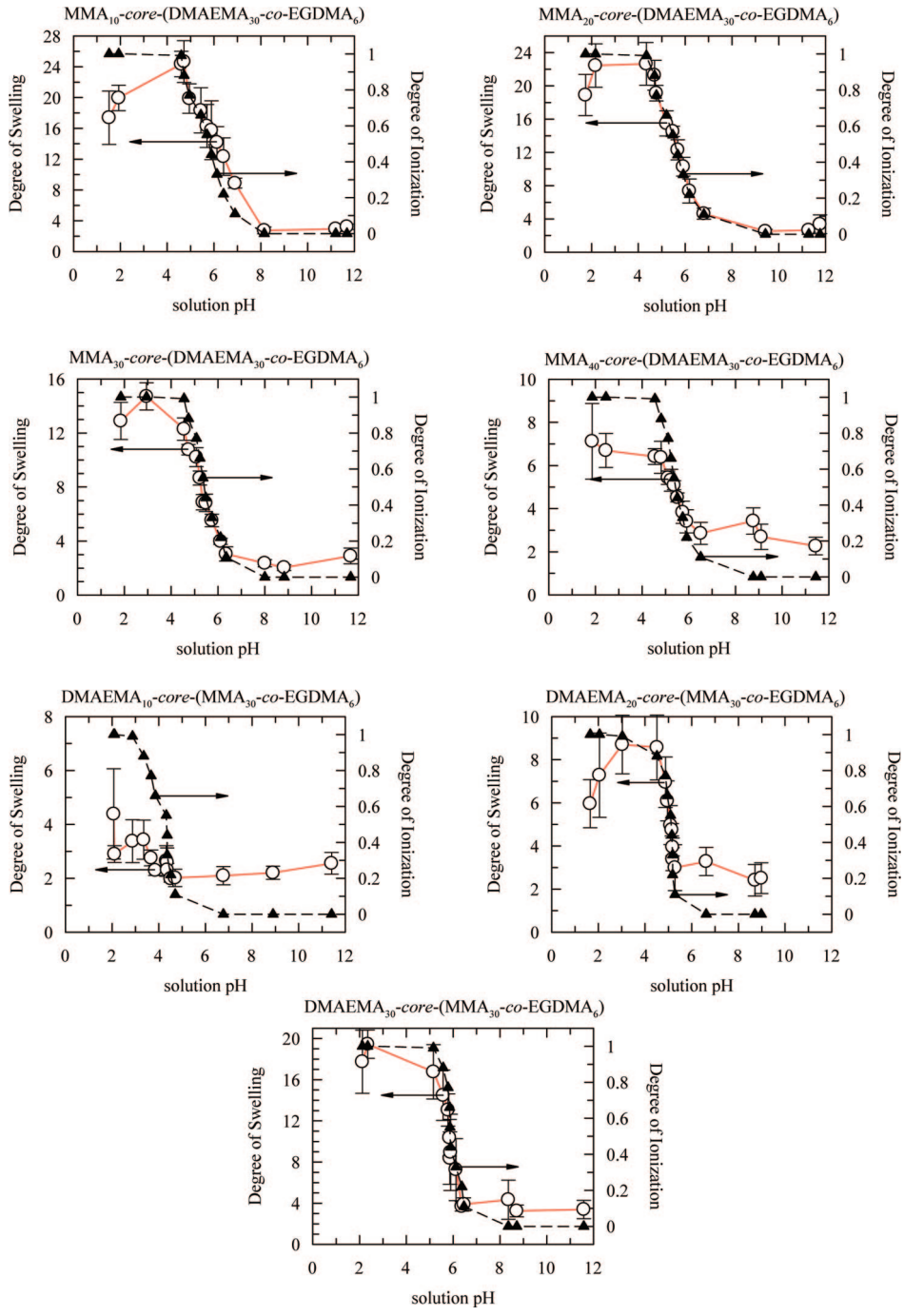

Figure 6. Aqueous degrees of swelling and degrees of ionization of the APCNs as a function of the solution pH.

units at 3.58 ppm (three protons). The experimental DMAEMA compositions of the extractables from the conetworks with polyMMA arms were much lower than the corresponding theoretical values because the sol fraction of these conetworks was substantially enriched with a large amount of linear polyMMA chains, but they were in good agreement with the "corrected theoretical" compositions. For the same reason, the experimental DMAEMA compositions of the extractables from the conetworks with polyDMAEMA arms were much higher than the corresponding theoretical ones because the sol fraction of these conetworks consisted of a large amount of linear polyDMAEMA chains, and they were also in good agreement with the "corrected theoretical" compositions.

Degrees of Swelling. The DSs of the conetworks measured in THF are shown in Table 4. They depended on the architecture and composition of the conetwork. Although THF is a nonselective solvent for both the DMAEMA and the MMA units, the APCNs with polyMMA arms presented lower DSs than the conetworks with polyDMAEMA arms. This difference is consistent with the difference in the sol fraction of the conetworks. In particular, the APCNs with polyMMA arms had a lower sol fraction than those with polyDMAEMA arms. This may be reasonable because the polyDMAEMA arms are bulkier than the polyMMA arms, resulting in stronger steric hindrances. Therefore, the DMAEMA/EGDMA cross-linking mixture (i.e., conetworks with polyMMA arms) would be more efficient for conetwork formation than the MMA-based one. In both cases, an increase in the DP of the arms led to an increase in the DSs in THF. All conetworks were more swollen in THF than in high pH water. This was because THF was a good solvent for both DMAEMA and MMA, whereas alkaline water was a nonsolvent

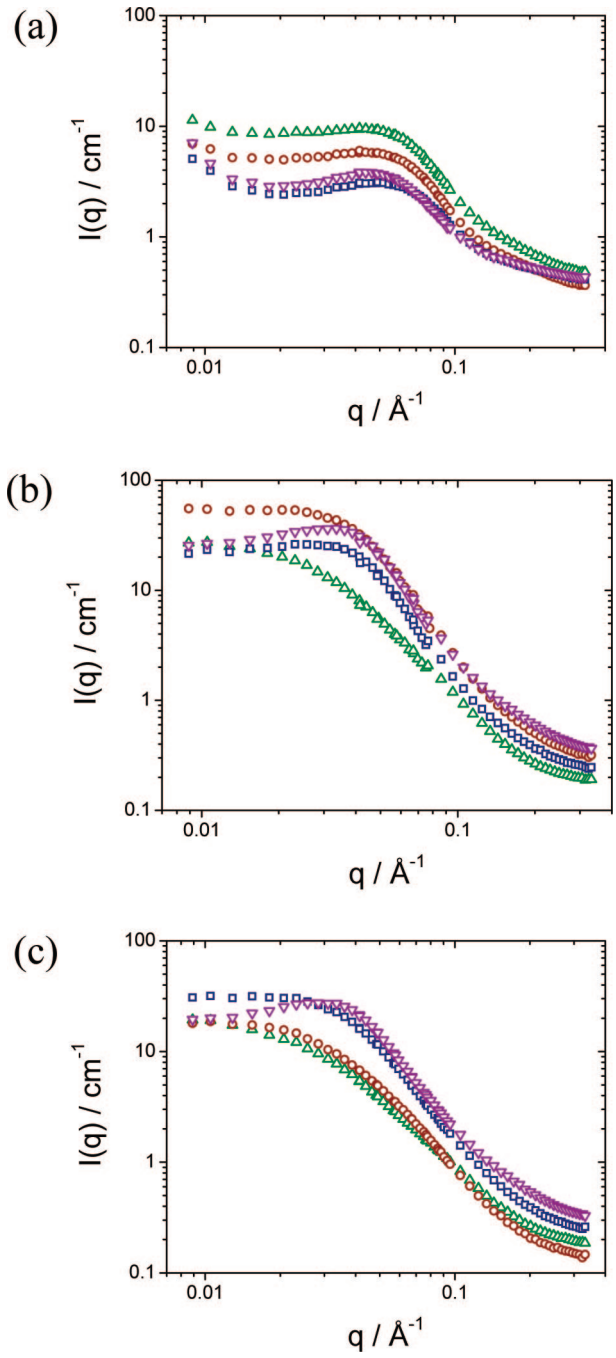

Figure 7. Neutron scattering profiles of the APCNs MMA$_n$-*core*-(DMAEMA$_{30}$-*co*-EGDMA$_6$) in (a) D_2O, (b) D_2O and 50% degree of ionization, and (c) D_2O and 100% degree of ionization with polyMMA arm DPs of 10 (△), 20 (○), 30 (□), and 40 (▽).

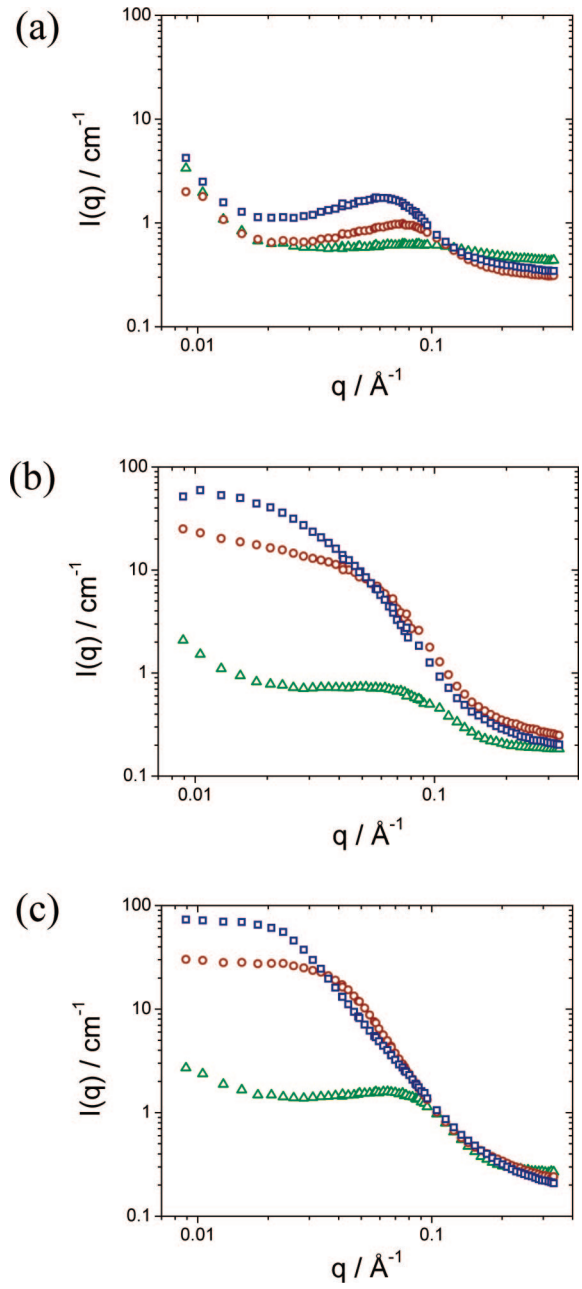

Figure 8. Neutron scattering profiles of the APCNs DMAEMA$_n$-*core*-(MMA$_{30}$-*co*-EGDMA$_6$) in (a) D_2O, (b) D_2O and 50% degree of ionization, and (c) D_2O and 100% degree of ionization with polyDMAEMA arm DPs of 10 (△), 20 (○), and 30 (□).

for the MMA units and an almost θ-solvent for the DMAEMA units.[23]

Figure 6 shows the pH dependence of the aqueous DSs and the degrees of ionization of the seven APCNs. At high pH values (pH > 7), where the DMAEMA units were not ionized, low DSs were obtained for all conetworks, suggesting a collapsed state, which is in agreement with previous studies on DMAEMA-MMA quasi-model conetworks.[18a,b,19a,b] An increase in the DS at low pH values (pH < 7) was observed because of the ionization of the DMAEMA residues,[24] which resulted in an increase in the osmotic pressure within the conetwork from the counterions to the charged DMAEMA units and in electrostatic repulsions between the charged polymer chains. These results are in agreement with previous work where an increase in the DS from high to low pH values was observed upon the ionization of the DMAEMA units in both homopolymer,[25] amphiphilic copolymer,[18a−d,f−h,j−l,19] and other functional DMAEMA-bearing copolymer conetworks.[26] The decrease in the DS of the conetworks below pH 2 could be attributed to the high ionic strength of the solution at this pH, conferred by the relatively high hydrochloric acid concentration, resulting in charge screening in the conetwork.[27]

As shown in Table 4 and Figure 6, and comparing the conetworks with the same composition in DMAEMA, the APCNs with polyDMAEMA arms displayed higher acidic DSs than those with polyMMA arms. This was because in the former type of conetwork, the hydrophilic DMAEMA was fully separated from the hydrophobic MMA and EGDMA components that were both located in the core of the conetwork, whereas in the latter, the core was a mixture of the hydrophilic DMAEMA and the hydrophobic cross-linker EGDMA. In this

Table 5. Calculated Spacing, *d*, between the Scattering Centers and Degrees of Swelling of the APCNs in the Deuterated SANS Solvents

	D_2O, 0% ionization		D_2O, 50% ionization		D_2O, 100% ionization	
polymer chemical formula[a]	*d* (Å)	DS	*d* (Å)	DS	*d* (Å)	DS
$DMAEMA_{10}$-*core*-(MMA_{30}-*co*-$EGDMA_6$)	73	2.2	109	2.5	109	3.4
$DMAEMA_{20}$-*core*-(MMA_{30}-*co*-$EGDMA_6$)	82	2.4	151	5.4	–	6.9
$DMAEMA_{30}$-*core*-(MMA_{30}-*co*-$EGDMA_6$)	109	1.9	–	8.4	–	14.5
MMA_{10}-*core*-($DMAEMA_{30}$-*co*-$EGDMA_6$)	151	3.4	–	20.9	–	29.4
MMA_{20}-*core*-($DMAEMA_{30}$-*co*-$EGDMA_6$)	151	2.4	303	14.4	–	28.4
MMA_{30}-*core*-($DMAEMA_{30}$-*co*-$EGDMA_6$)	151	2.4	271	6.4	408	15.0
MMA_{40}-*core*-($DMAEMA_{30}$-*co*-$EGDMA_6$)	151	2.2	187	4.4	221	6.6

[a] *core*: precedes the contents of the core of the APCNs.

latter case, swelling is reduced as a result of a reduction in the effective hydrophilicity of the DMAEMA units due to their mixing with the hydrophobic EGDMA units but also as a result of the restriction in the stretching of the polyDMAEMA segments due to their fragmentation by the EGDMA cross-linker units. In contrast, at high pH values, all conetworks had similar DSs of about 3. The DSs of the APCNs with polyMMA arms decreased as the DP of the arms increased because of the increase in the hydrophobicity of the conetwork and possible nanophase separation (see next section) within the conetwork. The highest acidic DS of the APCNs was obtained for the conetwork MMA_{10}-*core*-($DMAEMA_{30}$-*co*-$EGDMA_6$), which contained the lowest percentage of MMA and was, therefore, the most hydrophilic, whereas the lowest acidic DS was obtained for the conetwork MMA_{40}-*core*-($DMAEMA_{30}$-*co*-$EGDMA_6$), which bore the highest percentage of MMA and was the most hydrophobic.

In the case of the semisegmented APCNs with polyDMAEMA arms, an increase in the DP of the arms caused an increase in the acidic DS because of the increase in the hydrophilicity of the conetwork. For these APCNs, the lowest acidic DS was obtained for the conetwork $DMAEMA_{10}$-*core*-(MMA_{30}-*co*-$EGDMA_6$), which bore the lowest percentage of DMAEMA and was the most hydrophobic, whereas the highest acidic DS was obtained for the conetwork $DMAEMA_{30}$-*core*-(MMA_{30}-*co*-$EGDMA_6$), which contained the highest percentage of DMAEMA and was the most hydrophilic.

Structural Characterization. Figures 7 and 8 present the SANS profiles of all semisegmented APCNs of this study in deuterated water, where various precalculated volumes of a DCl solution in D_2O had been added to adjust the DMAEMA units in the conetworks to different degrees of ionization: 0, 50, and 100%. From these SANS profiles, important information about the nanostructural organization of the semisegmented APCNs was extracted, and it is discussed below.

Figure 7 shows the SANS profiles of the semisegmented APCNs with polyMMA arms (dangling chains) with DPs of 10, 20, 30, and 40. Figure 7a presents the scattering curves for all APCNs in pure D_2O (no added DCl, 0% degree of ionization of the DMAEMA monomer repeating units), which displayed a clear, albeit shallow, scattering peak, indicating a strong correlation between the scattering centers and suggesting nanophase separation. The scattering intensity at the peak maximum decreased with increasing length of the polyMMA arms, whereas the peak position was barely affected, implying that the mean spacing between the domains remained constant. Therefore, despite their semisegmented nature, the present APCNs self-organize in aqueous media, similar to their more perfect APCN counterparts based on end-linked amphiphilic ABA triblock copolymers.[18e] It is noteworthy that APCNs based on end-linked amphiphilic statistical copolymers (hydrophobic and hydrophilic monomers randomly distributed) or randomly cross-linked APCNs (with the two comonomers as well as the cross-linker randomly distributed) do not exhibit correlation peaks in their SANS profiles in D_2O.[18e]

At higher degrees of ionization of the DMAEMA units (Figure 7b,c), SANS correlation peaks persisted for the most hydrophobic APCNs but became broader and were shifted to lower q values, the more so the higher the degree of ionization. The last observation indicated the spacing out of the scattering centers and was also consistent with the higher DSs of the APCNs at higher degrees of ionization of the DMAEMA units. Note that the DSs in D_2O of the APCNs in the SANS study were directly measured (listed in Table 5) and were found to agree well with those in H_2O (Table 4).

In contrast, for the more hydrophilic conetworks with polyMMA DPs of 10 and 20 the peak became a shoulder or disappears when the degree of ionization of the DMAEMA units is increased. Therefore, the introduction of charge in these less hydrophobic conetworks weakened or destroyed the ordering in the structures.

Figure 8focuses on the SANS profiles of the semisegmented APCNs with polyDMAEMA arms with DPs of 10, 20, and 30. The trends are qualitatively somewhat similar to those in Figure 7 for the APCNs with polyMMA arms; therefore, similar interpretations can be given. In brief, there was indication for nanophase separation within all APCNs with polyDMAEMA arms when uncharged in D_2O, and this structural organization was preserved for the most hydrophobic APCN, even at full ionization of the DMAEMA units. However, in the uncharged state, these APCNs exhibited a clear shift of the correlation peak to larger spacings of the domains with increasing length of the polyDMAEMA arms, which was to be expected because such longer arms allowed for larger separation. At the same time, the domains became somewhat larger, as indicated by the increasing scattering intensity.

This effect of increasing scattering intensity became much more pronounced upon the ionization of the conetworks. (Compare part a with parts b and c of Figure 8.) Here a much different behavior between the sample with arms with DP 10 and the other two samples was evident.

Table 5shows the spacing between the scattering centers, *d*, which was estimated from the position of the intensity maximum, q_{max}, to be $2\pi/q_{max}$, or the position of the shoulder in some cases. As already mentioned, the Table also lists the DSs of the APCNs in deuterated water, where the SANS measurements were performed. Table 5 shows that the *d* values in D_2O span a range between 11 and 41 nm, increasing with the APCN DMAEMA content and the degree of ionization of the DMAEMA units, just as the DSs listed in the same Table.

Conclusions

GTP was used to prepare several semisegmented amphiphilic polymer conetworks based on the hydrophobic MMA and the hydrophilic DMAEMA in a two-step synthetic procedure. The first step involved the synthesis of well-defined linear polyDMAEMA or polyMMA arms, whereas in the second and final step, the second comonomer (the hydrophobic or the hydrophilic, respectively) was simultaneously copolymerized with the cross-linker, to form the main body of the conetwork, which was decorated with the dan-

gling chains prepared in step one. The cross-linking of the polyDMAEMA arms with a DP of 40 yielded an amphiphilic star copolymer. The size of the star copolymer was determined in solution using GPC-RI, GPC-SLS, DLS, and SANS and upon adsorption on a graphite surface using atomic force microscopy. The sol fraction extracted from the conetworks and the percentage of linear polymer in the sol fraction increased with the DP of the arms. The DSs in THF and in acidic water of the semisegmented APCNs with polyDMAEMA arms were higher than those of the conetworks with polyMMA arms. The aqueous DSs of the conetworks increased below pH 7 and increased with the composition in the hydrophilic monomer. Despite their less well-defined comonomer distribution compared with conetworks based on end-linked block copolymers, these semisegmented amphiphilic conetworks also nanophase separated in deuterated water, as revealed by SANS. The spacing of the SANS scattering centers followed the DSs, increasing with conetwork hydrophilicity and degree of ionization.

Acknowledgment. We thank the University of Cyprus Research Committee (grant 2004-2007) for the financial support for this work and contributing together with the Cyprus Research Promotion Foundation (project TEXNO/0104/13) to the purchase of the atomic force microscope used in this investigation. The A. G. Leventis Foundation is also thanked for a generous donation that enabled the purchase of the NMR spectrometer of the University of Cyprus. The Laboratoire Léon Brillouin, CEA-Saclay, France, and the European Union are also thanked for funding the SANS experiments. The valuable and comprehensive help of Dr. Laurence Noirez with the SANS experiments is gratefully acknowledged.

References and Notes

(1) (a) Patrickios, C. S.; Georgiou, T. K. *Curr. Opin. Colloid Interface Sci.* **2003**, *8*, 76–85. (b) Erdodi, G.; Kennedy, J. P. *Prog. Polym. Sci.* **2006**, *31*, 1–18. (c) Gitsov, I. *J. Polym. Sci., Part A: Polym. Chem.* **2008**, *46*, 5295–5314.

(2) (a) Zhu, C.; Hard, C.; Lin, C. P.; Gitsov, I. *J. Polym. Sci., Part A: Polym. Chem.* **2005**, *43*, 4017–4029. (b) Lequieu, W.; Du Prez, F. E. *Polymer* **2004**, *45*, 749–757. (c) Haraszti, M.; Tóth, E.; Iván, B. *Chem. Mater.* **2006**, *18*, 4952–4958. (d) He, C. J.; Erdödi, G.; Kennedy, J. P. *J. Polym. Sci., Part B: Polym. Phys.* **2006**, *44*, 1474–1481. (e) Haesslein, A.; Ueda, H.; Hacker, M. C.; Jo, S.; Ammon, D. M.; Borazjani, R. N.; Kunzler, J. F.; Salamone, J. C.; Mikos, A. G. *J. Controlled Release* **2006**, *114*, 251–260. (f) Sahli, N.; Belbachir, M.; Lutz, P. J. *Macromol. Chem. Phys.* **2005**, *206*, 1257–1270. (g) Doura, M.; Aota, H.; Matsumoto, A. *J. Polym. Sci., Part A: Polym. Chem.* **2004**, *42*, 2192–2201. (h) Guan, Y.; Ding, X. B.; Zhang, W. C.; Wan, G. X.; Peng, Y. X. *Macromol. Chem. Phys.* **2002**, *203*, 900–908. (i) Sun, Y.; Rimmer, S. *Ind. Eng. Chem. Res.* **2005**, *44*, 8621–8625. (j) Burns, N.; Tiller, J. C *Macromolecules* **2006**, *39*, 4386–4394. (k) Toman, L.; Janata, M.; Spěváček, J.; Brus, J.; Sikora, A.; Látalová, P.; Holler, P.; Vlček, P.; Dvořánková, B. *J. Polym. Sci., Part A: Polym. Chem.* **2006**, *44*, 6378–6384. (l) Powell, K. T.; Cheng, C.; Wooley, K. L.; Singh, A.; Urban, M. W. *J. Polym. Sci., Part A: Polym. Chem.* **2006**, *44*, 4782–4794. (m) Bromberg, L.; Temchenko, M.; Hatton, T. A. *Langmuir* **2002**, *18*, 4944–4952.

(3) (a) Vamvakaki, M.; Patrickios, C. S. *J. Phys. Chem. B* **2001**, *105*, 4979–4986. (b) Georgiou, T. K.; Vamvakaki, M.; Patrickios, C. S. *Polymer* **2004**, *45*, 7341–7355. (c) Karbarz, M.; Stojek, Z.; Patrickios, C. S. *Polymer* **2005**, *46*, 7456–7462. (d) Karbarz, M.; Stojek, Z.; Georgiou, T. K.; Patrickios, C. S. *Polymer* **2006**, *47*, 5182–5186.

(4) Barakat, I.; Dubois, Ph.; Grandfils, Ch.; Jérôme, R. *J. Polym. Sci., Part. A: Polym. Chem.* **1999**, *37*, 2401–2411.

(5) Behravesh, E.; Jo, S.; Zygourakis, K.; Mikos, A. G. *Biomacromolecules* **2002**, *3*, 374–381.

(6) Bruns, N.; Tiller, J. C. *Nano Lett.* **2005**, *5*, 45–48.

(7) Hentze, H.-P.; Krämer, E.; Berton, B.; Förster, S.; Antonietti, M.; Dreja, M. *Macromolecules* **1999**, *32*, 5803–5809.

(8) Scherble, J.; Thomann, R.; Iván, B.; Mülhaupt, R. *J. Polym. Sci., Part B: Polym. Phys.* **2001**, *39*, 1429–1436.

(9) Nicolson, P. C.; Vogt, J. *Biomaterials* **2001**, *22*, 3273–3283.

(10) Du Prez, F. E.; Goethals, E. J.; Schué, R.; Qariouh, H.; Schué, F. *Polym. Int.* **1998**, *46*, 117–125.

(11) Reyntjens, W.; Jonckheere, L.; Goethals, E. J.; Du Prez, F. *Macromol. Symp.* **2001**, *164*, 293–300.

(12) Hanko, M.; Bruns, N.; Tiller, J. C.; Heinze, J. *Anal. Bioanal. Chem.* **2006**, *386*, 1273–1283.

(13) (a) Bruns, N.; Bannwarth, W.; Tiller, J. C. *Biotechnol. Bioeng.* **2008**, *101*, 19–26. (b) Hensle, E. M.; Tobis, J.; Tiller, J. C.; Bannwarth, W. *J. Fluorine Chem.* **2008**, *129*, 968–973.

(14) (a) Hild, G. *Prog. Polym. Sci.* **1998**, *23*, 1019–1149. (b) Malkoch, M.; Vestberg, R.; Gupta, N.; Mespouille, L.; Dubois, P.; Mason, A. F.; Hedrick, J. L.; Liao, Q.; Frank, C. W.; Kingsbury, K.; Hawker, C. J. *Chem. Commun.* **2006**, 2774–2776. (c) Johnson, J. A.; Lewis, D. R.; Díaz, D. D.; Finn, M. G.; Koberstein, J. T.; Turro, N. J. *J. Am. Chem. Soc.* **2006**, *128*, 6564–6565. (d) Johnson, J. A.; Finn, M. G.; Koberstein, J. T.; Turro, N. J. *Macromolecules* **2007**, *40*, 3589–3598. (e) Johnson, J. A.; Baskin, J. M.; Bertozzi, C. R.; Koberstein, J. T.; Turro, N. J. *Chem. Commun.* **2008**, 3064–3066.

(15) Triftaridou, A. I.; Kafouris, D.; Vamvakaki, M.; Georgiou, T. K.; Krasia, T. C.; Themistou, E.; Hadjiantoniou, N.; Patrickios, C. S. *Polym. Bull.* **2007**, *58*, 185–190.

(16) (a) Webster, O. W.; Hertler, W. R.; Sogah, D. Y.; Farnham, W. B.; RajanBabu, T. V. *J. Am. Chem. Soc.* **1983**, *105*, 5706–5708. (b) Sogah, D. Y.; Hertler, W. R.; Webster, O. W.; Cohen, G. M. *Macromolecules* **1987**, *20*, 1473–1488. (c) Dicker, I. B.; Cohen, G. M.; Farnham, W. B.; Hertler, W. R.; Laganis, E. D.; Sogah, D. Y. *Macromolecules* **1990**, *23*, 4034–4041. (d) Webster, O. W. *J. Polym. Sci., Part A: Polym. Chem.* **2000**, *38*, 2855–2860. (e) Webster, O. W. *Adv. Polym. Sci.* **2004**, *167*, 1–34.

(17) (a) Chiefari, J.; Chong, Y. K.; Ercole, F.; Krstina, J.; Jeffery, J.; Le, T. P. T.; Mayadunne, R. T. A.; Meijs, G. F.; Moad, C. L.; Moad, G.; Rizzardo, E.; Thang, S. H. *Macromolecules* **1998**, *31*, 5559–5562. (b) Moad, G.; Rizzardo, E.; Thang, S. H. *Aust. J. Chem.* **2005**, *58*, 379–410. (c) Moad, G.; Rizzardo, E.; Thang, S. H. *Aust. J. Chem.* **2006**, *59*, 669–692. (d) Barner-Kowollik, C.; Davis, T. P.; Stenzel, M. H. *Aust. J. Chem.* **2006**, *59*, 719–727. (e) Lowe, A. B.; McCormick, C. L. *Prog. Polym. Sci.* **2007**, *32*, 283–351.

(18) (a) Simmons, M. R.; Yamasaki, E. N.; Patrickios, C. S. *Macromolecules* **2000**, *33*, 3176–3179. (b) Triftaridou, A. I.; Hadjiyannakou, S. C.; Vamvakaki, M.; Patrickios, C. S. *Macromolecules* **2002**, *35*, 2506–2513. (c) Hadjiantoniou, N.; Triftaridou, A. I.; Georgiou, T. K.; Patrickios, C. S. *Macromol. Symp.* **2005**, *227*, 135–142. (d) Krasia, T. C.; Patrickios, C. S. *Macromolecules* **2006**, *39*, 2467–2473. (e) Kali, G.; Georgiou, T. K.; Iván, B.; Patrickios, C. S.; Loizou, E.; Thomann, Y.; Tiller, J. C. *Macromolecules* **2007**, *40*, 2192–2200. (f) Georgiou, T. K.; Patrickios, C. S.; Groh, P. W.; Iván, B. *Macromolecules* **2007**, *40*, 2335–2343. (g) Triftaridou, A. I.; Vamvakaki, M.; Patrickios, C. S. *Biomacromolecules* **2007**, *8*, 1615–1623. (h) Achilleos, M.; Krasia-Christoforou, T.; Patrickios, C. S. *Macromolecules* **2007**, *40*, 5575–5581. (i) Kali, G.; Georgiou, T. K.; Iván, B.; Patrickios, C. S.; Loizou, E.; Thomann, Y.; Tiller, J. C. *Langmuir* **2007**, *23*, 10746–10755. (j) Hadjiantoniou, N. A.; Patrickios, C. S. *Polymer* **2007**, *48*, 7041–7048. (k) Vamvakaki, M.; Patrickios, C. S. *Soft Matter* **2008**, *4*, 268–276. (l) Triftaridou, A. I.; Loizou, E.; Patrickios, C. S. *J. Polym. Sci., Part A: Polym. Chem.* **2008**, *46*, 4420–4432. (m) Achilleos, M.; Legge, T. M.; Perrier, S.; Patrickios, C. S. *J. Polym. Sci., Part A: Polym. Chem.* **2008**, *46*, 7556–7565.

(19) (a) Vamvakaki, M.; Patrickios, C. S. *Chem. Mater.* **2002**, *14*, 1630–1638. (b) Achilleos, D. S.; Georgiou, T. K.; Patrickios, C. S. *Biomacromolecules* **2006**, *7*, 3396–3405. (c) Vamvakaki, M.; Patrickios, C. S.; Lindner, P.; Gradzielski, M. *Langmuir* **2007**, *23*, 10433–10437.

(20) Cotton, J. P. In *Neutron, X-ray, and Light Scattering: Introduction to an Investigative Tool for Colloidal and Polymeric Systmes*; Lindner, P., Zemb, Th., Eds.; North-Holland: Amsterdam, 1991; p 19.

(21) Benoit, H. *J. Polym. Sci.* **1953**, *11*, 507.

(22) Rempp, P.; Merrill, E. W. Chapter 5. *Polymer Synthesis*, 2nd ed.; Hüthig & Wepf: Basel, Switzerland, 1991; pp 122−126.

(23) Baines, F. L.; Billingham, N. C.; Armes, S. P. *Macromolecules* **1996**, *29*, 3416–3420.

(24) Siegel, R. A.; Firestone, B. A. *Macromolecules* **1988**, *21*, 3254–3259.

(25) (a) Costa, C. N.; Patrickios, C. S. *J. Polym. Sci., Part A: Polym. Chem.* **1999**, *37*, 1597–1607. (b) Simmons, M. R.; Yamasaki, E. N.; Patrickios, C. S. *Polymer* **2000**, *41*, 8523–8529. (c) Hadjiyannakou, S. C.; Yamasaki, E. N.; Patrickios, C. S. *Polymer* **2001**, *42*, 9205–9209. (d) Vamvakaki, M.; Yamasaki, E. N.; Hadjiyannakou, S. C.; Patrickios, C. S. *Macromol. Symp.* **2001**, *171*, 209–224.

(26) (a) Demosthenous, E.; Hadjiyannakou, S. C.; Vamvakaki, M.; Patrickios, C. S. *Macromolecules* **2002**, *35*, 2252–2260. (b) Loizou, E.; Triftaridou, A. I.; Georgiou, T. K.; Vamvakaki, M.; Patrickios, C. S. *Biomacromolecules* **2003**, *4*, 1150–1160. (c) Georgiou, T. K.; Patrickios, C. S. *Biomacromolecules* **2008**, *9*, 574–582.

(27) Philippova, O. E.; Hourdet, D.; Audebert, R.; Khokhlov, A. R. *Macromolecules* **1997**, *30*, 8278–8285.

MA802859D